Optical method for verification of homogeneity of phantoms for calibration of magnetic resonance

A. Sękowska, [1,2] A. Kamińska,[1] and A. Sabisz[3]

[1]*Department of Metrology and Optoelectronics, Faculty of Electronics, Telecommunications and Informatics, Gdańsk University of Technology, G. Narutowicza 11/12, Gdańsk,*
[2]*Department of Medical Physics, Pomeranian Medical University, Ku Słońcu 12, Szczecin,*
[3]*2-nd Department of Radiology, Medical University of Gdansk, M. Skłodowskiej-Curie 3, Gdańsk*

Received August 24, 2018; accepted September 05, 2018; published September 30, 2018

Abstract—The primary purpose of this study was to develop a laboratory photonic set-up for characterisation of homogeneity of gel phantoms for calibration of magnetic resonance. In this system, optical coherence tomography allows the detection of micro- and macroscopic heterogeneities of a structure. The set-up was used to perform measurements of agar and agar-carrageenan gels, which are the basis for more complex phantoms for magnetic resonance calibration. Obtained results were compared with magnetic resonance tomography methods used to detect macroscopic spatial differences in composition and heterogeneity in phantoms.

Magnetic resonance imaging (MRI) is a commonly used and, importantly, non-invasive method to illustrate normal tissues and pathological changes inside the human body. Nevertheless, before a new MRI device is approved for use, it is necessary to calibrate it properly and check the compatibility of its technical parameters with the manufacturer's specification. In order to do that, various calibration phantoms are created [1-2] - some of them are used to determine geometric accuracy, others to calibrate relaxation times and proton density.

Manufacturing procedures of new phantoms for calibration of medical devices are still being developed [3-8]. Unfortunately, in the production process different heterogeneities may emerge, such as air bubbles or spatial differences in the composition. The occurrence of such impurities is at first verified visually, however, some may not be visible to the naked eye. In the case of phantoms for calibration of magnetic resonance those heterogeneities may change relaxation times locally, which evident in T_1- and T_2- weighted images, and disturb the measurement of its averaged value. Therefore, in this study we investigate the possibility of detecting heterogeneities occurring in phantoms by means of optical coherence tomography.

Phantoms for calibration of relaxation times are usually prepared on the basis of aqueous suspensions or agarose gels. Occasionally, polyvinyl alcohol (PVA), gelatine, modified polysaccharide gels (TX-150 and TX-151) and carrageenan are also used [7]. For the purpose of this research, a set of base phantoms was created [9] – agar and agar-carrageenan gels varying in composition. An appropriate portion of agar and carrageenan was weighed into the beaker. Then, distilled water was added to obtain the desired volume. The resulting suspension was heated in an autoclave to completely dissolve the gelling agents. Hot liquid gels were poured into applicable containers. Table 1 presents the composition of prepared agar and agar-carrageenan gels.

Table 1. Quantitative composition of produced phantoms.

Phantom number	Agar content [g/100ml]	Carrageenan content [g/100ml]
1	1.272	2.000
2	1.413	2.000
3	1.554	2.000
4	1.272	0.000
5	1.413	0.000
6	1.554	0.000

Initial quality assessment of prepared phantoms has been investigated with the use of swept source optical coherence tomography (SS-OCT) [10]. This technique enables the detection of defects in the internal structure through the measurement of back radiation intensity scattered by heterogeneities in the examined object [11]. Moreover, this method allows obtaining cross-sectional images of the studied object with a micrometer resolution. The principle of SS-OCT operation has been presented in Fig. 1.

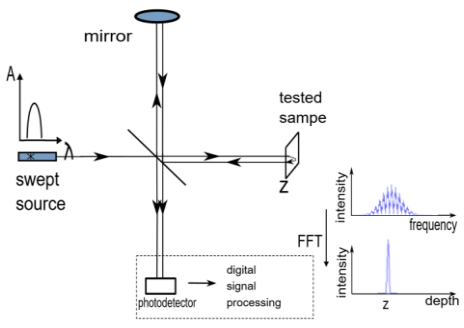

Fig. 1. The SS-OCT system set-up, where *z* is the depth of the reflecting layer.

The properties of the applied OCT system are presented in Table 2.

Table 2. Properties of the OCT system.

Item	Value
light source type	20 kHz swept source
average output power	10 [mW]
central wavelength	1320 [nm]
wavelength range	140 [nm]
axial resolution	12 [μm]
lateral resolution	15 [μm]
frame rate	> 4 [fps]
max. depth imaging range / transverse imaging range	7 / 10 [mm]

Sample 2D images of the internal structure of phantoms 2 and 5 obtained by optical coherence tomography are presented in Fig. 2a and 2b.

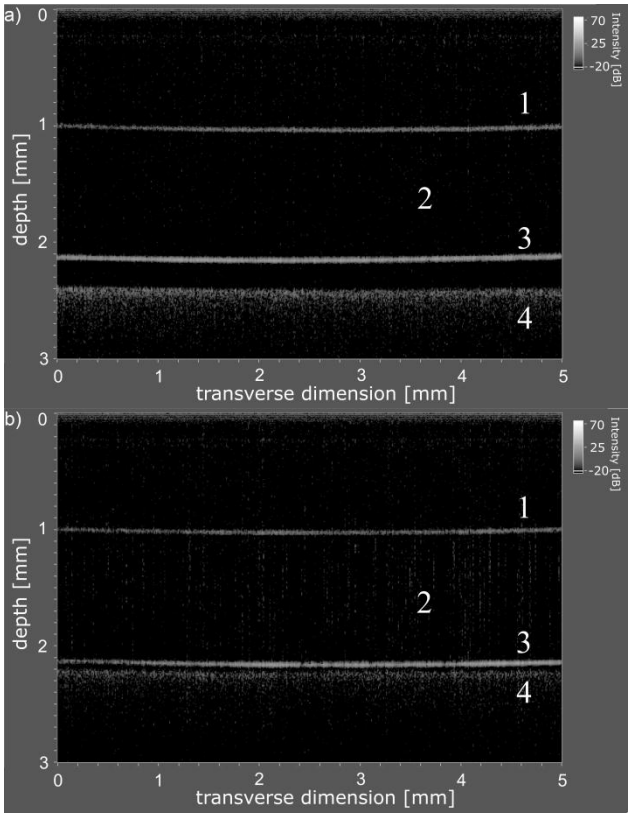

Fig. 2. OCT images of agar gel (a, phantom № 5) and agar-carrageenan gel (b, phantom № 2), where 1- sample surface, 2 - the interior of the sample, 3 - the bottom of the sample and Petri dish, 4 - noise from laboratory stage.

The OCT image of agar gel does not show any scattering centers, which proves the homogeneity of an internal structure. Adding carrageenan caused an increase in the heterogeneity. The OCT image shows grey points which indicate the occurrence of scattering centers. This may denote that the selected carrageenan concentration is too high to obtain a fully homogeneous gel structure.

Magnetic resonance imaging was performed with the Philips Achivea 3.0T-TX system using a 32-channel cardiac coil. The parameters of the applied MRI measurement sequence are presented in Table 3.

Tab. 3. Parameters of applied MRI sequence

Item	Value
scanning sequence	turbo spin echo
voxel size	0.375 × 0.375 [mm × mm]
slice thickness	3.00 [mm]
repetition time	400 (T_1-weighted image), 3000 (T_2-weighted) [ms]
echo time	8 (T_1-weighted image), 90 (T_2-weighted) [ms]

The results obtained by optical coherence tomography can be compared with the visual assessment of phantoms' structure based on T_1- and T_2-weighted images presented in Figs. 3 and 4. These are exemplary images of the prepared phantoms at the same slice position. On a T_2-weighted image, the higher the relaxation time, the brighter is the area. In the case of a T_1-weighted image the relationship is reversed.

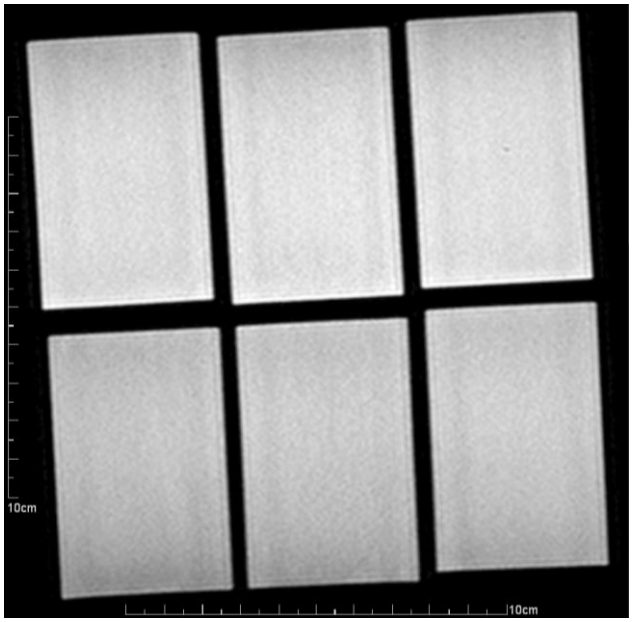

Fig. 3. T_1-weighted image of base phantoms; (1st row: phantoms № 1, 2, 3; 2nd row: phantoms № 4, 5, 6).

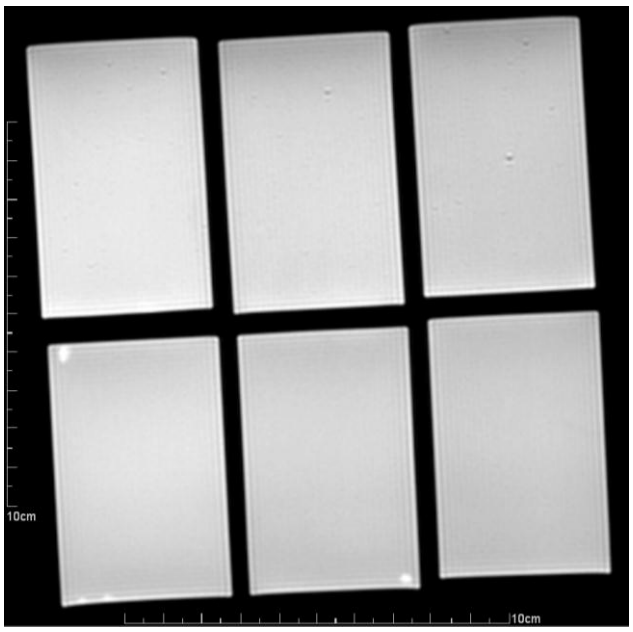

Fig. 4. T_2-weighted image of base phantoms;
(1st row: phantoms № 1, 2, 3; 2nd row: phantoms № 4, 5, 6)

Based on the obtained T_1- and T_2-weighted images, it is possible to visually assess the homogeneity of the base phantoms for magnetic resonance calibration. The following properties are to be assessed: occurrence of air bubbles, differences in phantom composition reflected in the form of streaks or local discoloration. The presented images show single air bubbles created in the agar-carrageenan phantoms and local discoloration of agar phantoms number 4 and 5, indicating the existence of local differences in the composition of those phantoms.
The study shows that the developed system allows the detection of heterogeneities and slight differences in the composition of MR calibration phantoms. The use of OCT in the preliminary assessment of homogeneity of phantoms will allow the exclusion of heterogeneous samples. Moreover, the developed method is more affordable and accessible.

This work was partially supported by the Centre for Knowledge and Technology Transfer as part of the project "Incubator of Innovation+". The DS funds of the Faculty of Electronics, Telecommunications, and Informatics of the Gdansk University of Technology are also acknowledged. The authors would like to thank prof. Edyta Szurowska of the Medical University of Gdańsk for allowing the measurements to be taken on Philips Achivea 3.0T-TX system.

References

[1] R.R. Price *et al*., Med. Phys. **17**(2), 287 (1990).
[2] P.S. Tofts, QA: quality assurance, accuracy, precision and phantoms in P.S. Tofts, *Quantitative MRI of the brain: measuring changes caused by disease* (Chichester: John Wiley, ISBN: 0-470-84721-2).
[3] M. Wróbel, A. Popov, A. Bykov, V.V. Tuchin, M. Jędrzejewska-Szczerska, Biomed. Opt. Expr. **7**(6), 2088 (2016).
[4] I. Feder, M. Wróbe, H. Duadi, M. Jędrzejewska-Szczerska, D. Fixler, Biomed. Opt. Expr. **7**(11), 4695 (2016).
[5] M.S. Wróbel *et al*., J. Biomed. Opt. **20**(8), 085003 (2015).
[6] M.S. Wróbel *et al*., J. Inn. Opt. Health Scien. **8**(3), 1541005-1 (2015).
[7] A. Hellerbach, V. Schuster, A. Jansen, J. Sommer, PLoS ONE 8(8): e70343; https://doi.org/10.1371/journal.pone.0070343.
[8] N.K. Almazrouei, M.I. Newton, E.R. Dye, R.H. Morris, MDPI Proceedings **2**, 122 (2018).
[9] S. Ohno *et al*., Magn. Reson. Med. Scien. **7**(3), 131 (2008).
[10] M.A. Choma, M.V. Sarunic, C. Yang, J.A. Izatt, Opt. Expr. **11**, 2183 (2003).
[11] M.R. Strąkowski, M. Głowacki, A. Kamińska, M. Sawczak, Proc. SPIE 10053, Optical Coherence Tomography and Coherence Domain Optical Methods in Biomedicine XXI, 1005336 (2017).

